Bloch Diode

M. Houzet,[1] T. Vakhtel,[2] and J. S. Meyer[1]
[1]Univ. Grenoble Alpes, CEA, Grenoble INP, IRIG, Pheliqs, F-38000 Grenoble, France
[2]QuTech and Kavli Institute of Nanoscience, Delft University of Technology, Delft 2628 CJ, The Netherlands

(Received 16 November 2025; accepted 12 March 2026; published 8 April 2026)

The Josephson diode effect—an asymmetry of critical currents at opposite polarities—has attracted much attention recently. One of its simplest realizations is an asymmetric SQUID with multiple Josephson harmonics tuned away from half-integer flux (in units of the superconducting flux quantum). Here we predict a dual version of this effect in a gate-tunable Cooper pair transistor placed in series with a highly resistive environment. The dual "Bloch diode effect" manifests itself as an asymmetry of critical voltages at opposite polarities when the Cooper pair transistor is tuned away from half-integer gate charge (in units of the Cooper pair charge). It arises from an asymmetry in the dispersion of the transistor's Bloch bands. A highly resistive environment can be realized with a Josephson junction array, suggesting that such a Bloch diode could be implemented using conventional superconducting quantum circuits.

DOI: 10.1103/q98p-j4vh

The Josephson diode effect is characterized by asymmetric critical currents for opposite directions of the current flow across a Josephson junction between two superconducting leads [1]. The breaking of both inversion and time-reversal symmetries is necessary to generate an equilibrium current-phase relation that displays such critical current asymmetry. Out of equilibrium, this asymmetry then results in a nonreciprocal current-voltage characteristic as the junction is embedded in a dissipative environment. In particular, the Josephson diode may be used as a ratchet, a device able to rectify a signal with a zero time average [2]. The interplay of magnetism and spin-orbit coupling provides a nontrivial contribution to the Josephson diode effect [3] and motivates the recent resurgence of interest in its study in Josephson junctions made with exotic materials [1]. Still, it has been known for a long time that Josephson diodes may also exist in the absence of spin-orbit coupling, provided that inversion symmetry is broken at a macroscopic rather than microscopic level [4]. In particular, they have been recently studied theoretically [5,6] and experimentally [7,8] in asymmetric superconducting quantum-interference devices (SQUIDs) with more than one harmonic in the current-phase relation of the Josephson junctions that constitute them.

Contrasting views about the role of Coulomb interaction on the nonreciprocal response of a Josephson junction have been presented. On the one hand, quantum fluctuations due to charging effects are detrimental to the Josephson diode effect described above [9,10]. Indeed, the latter is associated with an equilibrium current-phase relation that breaks parity symmetry, $I_J(-\varphi) \neq -I_J(\varphi)$. Now let us add to the Josephson potential $U(\varphi)$, such that $I_J = (2e/\hbar)\partial_\varphi U$, the standard Coulomb potential quadratic in the charge variable canonically conjugate to φ. Then, as is well known from quantum mechanics [11], the Bloch wave functions u_q of quasimomentum q for the resulting Hamiltonian remain symmetric under inversion of quasimomentum, $u_q = u_{-q}$, despite the asymmetry of the Josephson potential, $U(-\varphi) \neq U(\varphi)$. Introducing a dissipative environment to address the current-voltage characteristic, one eventually finds that this absence of chirality in turn results in the suppression of any nonreciprocal response at low temperature as soon as the resistance of the environment exceeds the resistance quantum and the phase remains quantum-mechanically delocalized [12]. On the other hand, nonreciprocity is ubiquitous in conventional semiconducting diodes, such as a pn junction, where Onsager relations are bypassed by charge redistribution at finite bias. This observation questions the necessity of breaking time-reversal symmetry already in equilibrium, like in a Josephson diode, in order to get a nonreciprocal current-voltage characteristic. In fact, nonreciprocity was predicted in various phenomenological models of Josephson junctions preserving time-reversal symmetry, such that $I_J(-\varphi) = -I_J(\varphi)$, together with a nonquadratic electrostatic potential due to imperfect screening in semiconducting areas of the device [13–15].

In this Letter we discuss a concrete Josephson circuit with broken inversion symmetry only (see Fig. 1) which allows for realizing a nonreciprocal current-voltage characteristic. We rely on the phase-charge duality predicted by Schmid [12] to propose that a Cooper pair (or Bloch) transistor [16–19] in series with a highly resistive environment realizes a dual version of the resistively shunted SQUID with multiple Josephson harmonics; see Fig. 2. In the dual regime, the critical current asymmetry in the conventional Josephson diode is replaced by an asymmetry

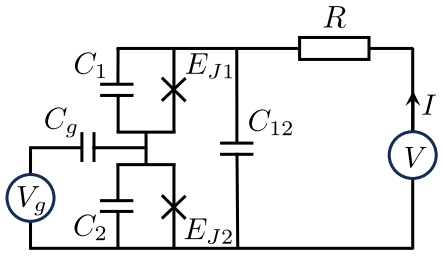

FIG. 1. The Bloch diode effect is predicted in a voltage-biased asymmetric Cooper pair transistor connected in series with a highly resistive environment, $R \gg R_Q$.

of critical voltages below which Coulomb blockade of Cooper pair tunneling takes place [20–24]. In our proposal, the breaking of inversion symmetry originates from an asymmetry either in charging or Josephson energy between the two Josephson junctions that form the Cooper pair transistor. At the same time, our proposal only requires an array of conventional metallic tunnel junctions. The nonreciprocal dc current that flows through the device is accompanied by an ac current that manifests Bloch oscillations, dual to the ac Josephson effect [25,26]. Therefore we suggest that the dual Josephson diode studied in this Letter should be dubbed the "Bloch diode." The recent observation of dual Shapiro steps induced by the mixing of microwaves with Bloch oscillations in voltage-biased single- and double-junction devices [27–29], which was enabled by their connection in series with a highly resistive environment, is encouraging for the observation of the Bloch diode effect.

At large environment resistance $R \gg R_Q$, where $R_Q = h/4e^2$ is the resistance quantum, the Cooper pair transistor in Fig. 1 behaves as a nonlinear capacitor [30,31]. The current-voltage characteristic of the circuit is then derived from the equation of motion,

$$V = RI + V_B(\mathcal{N}), \qquad V_B(\mathcal{N}) = -\frac{1}{2e}\frac{\partial \mathcal{E}_0}{\partial \mathcal{N}}, \tag{1}$$

which expresses the bias voltage V as the sum of the voltage drops at the resistor and at the effective nonlinear capacitor, respectively [16,25,26]. Here, the current $I = -2e\dot{\mathcal{N}}$ is related to the charge $\mathcal{N}$ (in units of the Cooper pair charge) displaced across the resistor, and $\mathcal{E}_0(\mathcal{N})$ is the ground-state energy of the Cooper pair transistor when it is electrostatically tunable. The (Bloch) voltage-charge relation $V_B(\mathcal{N})$ plays a dual role to the (Josephson) current-phase relation $I_J(\varphi)$, while the relation between I and $\dot{\mathcal{N}}$ mirrors the second Josephson relation between V and $\dot{\varphi}$.

Current is blocked in a voltage range $V_{c-} < V < V_{c+}$ with critical voltages

$$V_{c-} = \min_{\mathcal{N}} V_B(\mathcal{N}), \qquad V_{c+} = \max_{\mathcal{N}} V_B(\mathcal{N}). \tag{2}$$

Generically $V_{c-} \neq -V_{c+}$ for an asymmetric device. This asymmetry then develops into a nonreciprocal current-voltage characteristic beyond the blocked region. Below we determine the amplitude of this asymmetry by evaluating the so-called "dual diode efficiency,"

$$\eta = \frac{V_{c+} - |V_{c-}|}{V_{c+} + |V_{c-}|}, \tag{3}$$

with $\eta_{\max}$ defined as the maximum of $|\eta|$. To find $\mathcal{E}_0$ that appears in Eq. (1), we introduce the Hamiltonian that describes an electrostatically controlled Cooper pair transistor,

$$H = -E_{J1}\cos\varphi_1 - E_{J2}\cos\varphi_2 + E_{C1}(N_1 - \mathcal{N})^2 + E_{C2}(N_2 - \mathcal{N} - \mathcal{N}_g)^2 + E_{C0}(N_2 - N_1 - \mathcal{N}_g)^2. \tag{4}$$

Here φ_k and $-2eN_k$ are the canonically conjugate superconducting phase difference and Cooper pair charge that tunneled across the Josephson junction labeled by $k = 1, 2$, such that $[\varphi_k, N_{k'}] = i\delta_{k,k'}$, respectively. The two first terms in H describe Cooper-pair tunneling characterized by Josephson energies E_{J1} and E_{J2}. The last three terms involve external charges $\mathcal{N}$ and $\mathcal{N}_g = -C_g V_g/2e$ with gate capacitance C_g and gate voltage V_g, as well as charging energies $E_{C1} = 2e^2\tilde{C}_2/C_{\text{eff}}^2$, $E_{C2} = 2e^2 C_1/C_{\text{eff}}^2$, and $E_{C0} = 2e^2 C_{12}/C_{\text{eff}}^2$ with junction capacitances C_1 and C_2, cross-capacitance C_{12}, and $C_{\text{eff}}^2 = C_1\tilde{C}_2 + C_{12}(C_1 + \tilde{C}_2)$ with $\tilde{C}_2 = C_2 + C_g$. (From now on we replace $\tilde{C}_2$ with C_2 in all formulas assuming, e.g., $C_g \ll C_2$.)

Within this model, the asymmetry needed for a finite diode efficiency requires $C_1 \neq C_2$ or $E_{J1} \neq E_{J2}$. Furthermore, eigenfunctions $\Psi(\varphi_1, \varphi_2)$ of Eq. (4) are 2π-periodic in variables φ_1, φ_2. As a consequence, $\mathcal{E}_0$ is 1-periodic in variables $\mathcal{N}, \mathcal{N}_g$ and $\mathcal{E}_0(-\mathcal{N}, -\mathcal{N}_g) = \mathcal{E}_0(\mathcal{N}, \mathcal{N}_g)$. We deduce that the diode efficiency is an odd and 1-periodic function of variable $\mathcal{N}_g$, which vanishes if $\mathcal{N}_g = 0 \bmod \frac{1}{2}$. Thus we restrict our study to the range $0 < \mathcal{N}_g < \frac{1}{2}$.

We first consider the regime $C_{12} \ll C_1, C_2$ and ignore the last term in Eq. (4), such that the Hamiltonian becomes separable in variables (φ_1, N_1) and (φ_2, N_2). Then,

$$\mathcal{E}_0(\mathcal{N}, \mathcal{N}_g) = \mathcal{E}_1(\mathcal{N}) + \mathcal{E}_2(\mathcal{N} + \mathcal{N}_g), \tag{5}$$

where $\mathcal{E}_k(\mathcal{N})$ is the ground state energy of the Hamiltonian,

$$H_k = -E_{Jk}\cos\varphi_k + E_{Ck}(N_k - \mathcal{N})^2. \tag{6}$$

In particular,

$$\mathcal{E}_k(\mathcal{N}) \approx \begin{cases} \min_N E_{Ck}(\mathcal{N} - N)^2, & E_{Jk} \ll E_{Ck}, \\ \mathcal{E}_k^0 - \lambda_k \cos 2\pi\mathcal{N}, & E_{Jk} \gg E_{Ck}, \end{cases} \tag{7}$$

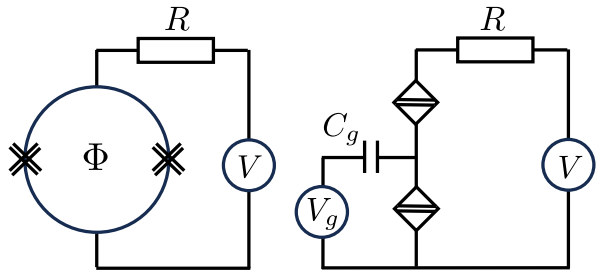

FIG. 2. Duality between the Josephson diode effect in a SQUID at $R \ll R_Q$ (left) and the Bloch diode effect in a Cooper pair transistor at $R \gg R_Q$ (right). The double cross represents a Josephson junction with multiple harmonics in its current-phase relation; the hatched diamond represents a quantum phase-slip junction with multiple harmonics in its voltage-charge relation. Time-reversal symmetry enforces $U(-\varphi,-\Phi)=U(\varphi,\Phi)$ for the Josephson potential of the SQUID, where Φ is the flux piercing the loop. Thus nonreciprocity is realized if Φ is tuned away from a half-integer flux (in units of the superconducting flux quantum) and the SQUID is asymmetric, such that $U(-\varphi,\Phi)\neq U(\varphi,\Phi)$. In the Cooper pair transistor, inversion symmetry enforces $\mathcal{E}_0(-\mathcal{N},-\mathcal{N}_g)=\mathcal{E}_0(\mathcal{N},\mathcal{N}_g)$ with $\mathcal{N}_g=-C_gV_g/2e$. Thus nonreciprocity is realized for two unequal phase-slip junctions if the gate charge is tuned away from a multiple of e, such that $\mathcal{E}_0(-\mathcal{N},\mathcal{N}_g)\neq\mathcal{E}_0(\mathcal{N},\mathcal{N}_g)$.

with $\mathcal{E}_k^0\approx -E_{Jk}+\frac{1}{2}\hbar\omega_k$; quantum phase slip amplitude,

$$\lambda_k=\frac{8}{\sqrt{\pi}}(2E_{Jk}^3E_{Ck})^{1/4}e^{-\sqrt{32E_{Jk}/E_{Ck}}}; \tag{8}$$

and Josephson plasma frequency $\omega_k=(1/\hbar)\sqrt{2E_{Jk}E_{Ck}}$ [32].

A single junction is not sufficient to obtain a diode. Thus, if the contribution of one of the two junctions dominates over the other one, say $\mathcal{E}_0\approx\mathcal{E}_1(\mathcal{N})$ for concreteness, then the diode efficiency vanishes. In that case, as the ratio E_{J1}/E_{C1} increases, $V_{c+}=-V_{c-}$ decreases from e/C_1 to $\pi\lambda_1/e$. By contrast, when both junctions provide comparable contributions to $\mathcal{E}_0$, the diode efficiency is finite. In particular, in the Coulomb dominated regime, assuming $C_1<C_2$ for concreteness, we find

$$\eta=\begin{cases}\frac{C_2-C_1}{C_1+C_2}\frac{\mathcal{N}_g}{1-\mathcal{N}_g}, & 0<\mathcal{N}_g<\frac{C_1}{C_1+C_2},\\ \frac{C_1}{C_2}(1-2\mathcal{N}_g), & \frac{C_1}{C_1+C_2}<\mathcal{N}_g<\frac{1}{2}.\end{cases} \tag{9}$$

The maximal diode efficiency, $\eta_{\max}=(\sqrt{2}-1)^2\simeq 0.17$, is reached at $C_1/C_2=\sqrt{2}-1$ and $\mathcal{N}_g=1-1/\sqrt{2}$.

In the Josephson dominated regime, by inserting the second line of Eq. (7) into Eq. (5), we find a modulation of the critical voltages,

$$V_{c\pm}^{J0}=\pm\frac{\pi}{e}\sqrt{(\lambda_1-\lambda_2)^2+4\lambda_1\lambda_2\cos^2\pi\mathcal{N}_g}, \tag{10}$$

(without diode effect) due to Aharonov-Casher (AC) interference [33,34], which is dual to the flux modulation of a SQUID. When $\lambda_1\approx\lambda_2$ and $\mathcal{N}_g\approx\frac{1}{2}$, the blocked region is suppressed. In that case, it is important to keep the next-to-leading order term [35,36] in the second line of Eq. (7) (see Appendix A for the derivation of its amplitude),

$$\mathcal{E}_k(\mathcal{N})\approx\mathcal{E}_k^0-\lambda_k\cos 2\pi\mathcal{N}+\frac{\lambda_k^2}{2\hbar\omega_k}\ln\left(\frac{2^4e^\gamma\hbar\omega_k}{E_{Ck}}\right)\cos 4\pi\mathcal{N}, \tag{11}$$

where γ is the Euler constant, to compute the critical voltage. (Note that the amplitude of that term, also called "double quantum phase slip" amplitude, was recently measured in a fluxonium qubit [37].) The dual diode effect then results from different AC-induced phase shifts in the first and second harmonics of the voltage-gate charge relation, similar to the case of a SQUID with higher harmonic content [5,6]. Following the analysis of Ref. [38] for the conventional Josephson diode effect, we find that the maximal dual diode efficiency, $\eta_{\max}=1/3$, is reached when

$$\frac{|\lambda_1-\lambda_2|}{\lambda_1}=\frac{\sqrt{2}\lambda_1}{\hbar\omega_1}\ln\left(\frac{E_{J1}}{E_{C1}}\right)=2\pi|\mathcal{N}_g-\frac{1}{2}|\ll 1, \tag{12}$$

corresponding to

$$\mathcal{E}_0(\mathcal{N})=\sqrt{2}|\lambda_1-\lambda_2|\left[\cos 2\pi\left(\mathcal{N}+\frac{1}{8}\right)+\frac{1}{4}\cos 4\pi\mathcal{N}\right]. \tag{13}$$

(Here we also assumed $\omega_1\approx\omega_2$ for simplicity.) The charge dispersion of $\mathcal{E}_0$ is illustrated in Fig. 3; it forms a ratchet potential. The asymmetry of critical voltages, $V_{c+}^J=-2V_{c-}^J=(3\pi/\sqrt{2})|\lambda_1-\lambda_2|/e$, is also seen in the voltage-charge relation.

The diode efficiency in a hybrid situation where one junction is in the Josephson dominated regime and the other

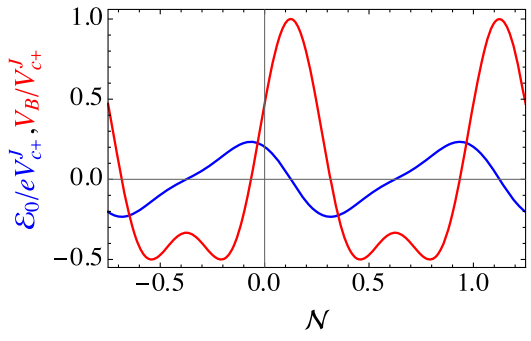

FIG. 3. Ratchet potential (blue) and voltage-charge relation (red) associated with a Bloch diode with efficiency $\eta=1/3$ in the Josephson-dominated regime, cf. Eq. (13).

one is in the Coulomb dominated regime is addressed in Appendix B.

Let us now consider the case when the Hamiltonian (4) is not separable. We first consider the case when E_{C0} dominates over all other energy scales, $E_{C0} \approx 2e^2/(C_1 + C_2) \gg E_{C1}, E_{C2}$ at $C_{12} \gg C_1, C_2$. Then charge in the central island is strongly pinned, and transport can only occur in the vicinity of a degeneracy point between two charge states. For concreteness, we consider $|\mathcal{N}_g - \frac{1}{2}| \ll 1$ and project the Hamiltonian (4) onto the charge basis with $N_2 - N_1 = 0, 1$. Then,

$$H = E_C\left(N - \mathcal{N} + \frac{\delta E_C}{4E_C}\sigma_z\right)^2 - E_{C0}\left(\frac{1}{2} - \mathcal{N}_g\right)\sigma_z - E_J\cos\frac{\varphi}{2}\sigma_x + \delta E_J \sin\frac{\varphi}{2}\sigma_y \tag{14}$$

(up to irrelevant constants). Here we introduced Pauli matrices in the basis of the two charge states of the island, and canonically conjugate variables $\varphi = \varphi_1 + \varphi_2$ and $N = (N_1 + N_2)/2$. Furthermore, $E_C = E_{C1} + E_{C2}$, $\delta E_C = E_{C1} - E_{C2}$, $E_J = (E_{J1} + E_{J2})/2$, and $\delta E_J = (E_{J1} - E_{J2})/2$. Charge conservation imposes the twisted boundary condition $\Psi(\varphi + 2\pi) = \sigma_z\Psi(\varphi)$ on eigenstates of Eq. (14) [39]. As discussed recently [40], Hamiltonian (14) has the same form as the Hamiltonian for a discrete resonant level coupled to superconducting leads at weak Coulomb interaction [39,41,42].

In the Coulomb dominated regime, $\sigma_z = \pm 1$ and $\mathcal{E}_0 = \min(\mathcal{E}_+, \mathcal{E}_-)$ with

$$\frac{\mathcal{E}_\pm}{E_C} = \min_{n\in\mathbb{Z}}\left(n - \mathcal{N} \mp \frac{\delta}{4} + \frac{1 \mp 1}{4}\right)^2 \pm \varepsilon, \tag{15}$$

$\delta = \delta E_C/E_C$, and $\varepsilon = E_{C0}(\frac{1}{2} - \mathcal{N}_g)/E_C$. As before we consider $C_1 < C_2$ corresponding to $\delta > 0$, where we find the diode efficiency,

$$\eta = \begin{cases} \frac{8\varepsilon}{(1+\delta)^2}, & 0 < \varepsilon < \frac{\delta}{8}(1-\delta^2), \\ \delta\frac{1-\delta^2-8\varepsilon}{1-\delta^2+8\varepsilon}, & \frac{\delta}{8}(1-\delta^2) < \varepsilon < \frac{1}{8}(1-\delta^2). \end{cases} \tag{16}$$

At $\varepsilon > \frac{1}{8}(1-\delta^2)$, the energies $\mathcal{E}_\pm$ do not cross and the diode efficiency vanishes. Equation (16) yields the same diode efficiency as in the separable case, $\eta_{\max} = (\sqrt{2}-1)^2$, which is realized at $\delta = \sqrt{2}-1$ and $\varepsilon = (\sqrt{2}-1)^2/4$. In fact, the result for $\eta_{\max} = (\sqrt{2}-1)^2$ holds in the Coulomb dominated regime even without assuming $C_{12} \gg C_1, C_2$. In that case, $\varepsilon = C_{\text{eff}}^2/(C_1 + C_2)^2(\frac{1}{2} - \mathcal{N}_g)$. The $\mathcal{N}$-dependence of $\mathcal{E}_0$ and charge-voltage relation at maximal diode efficiency, with $V_{c+}^C = -\sqrt{2}V_{c-}^C = (\sqrt{2}-1)E_C/e$, are shown in Fig. 4.

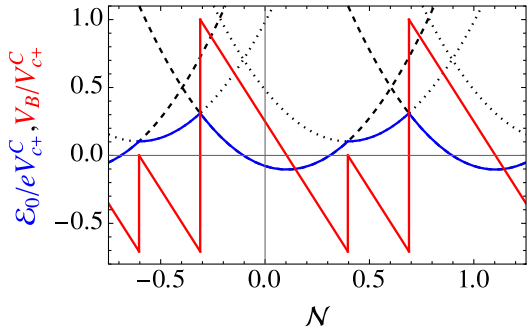

FIG. 4. Ratchet potential (blue) and voltage-charge relation (red) associated with a Bloch diode with efficiency $\eta = (\sqrt{2}-1)^2$ in the Coulomb-dominated regime. Dashed and dotted lines are metastable energies at fixed charge and $\sigma_z = \mp 1$, respectively, cf. Eq. (15). The gaps of the order $E_J \ll E_C$ when charging energies cross each other, and associated smearing of the charge-voltage relation, are not shown.

In the Josephson dominated regime, the Wentzel-Kramers-Brillouin (WKB) approximation was used to calculate the two first harmonics in the $\mathcal{N}$-dispersion of $\mathcal{E}_0$ at $C_{12} \gg C_1 = C_2$ [see Eqs. (19) and (25) in Ref. [39]], where the difference between AC shifts in the first and second harmonics in $2\pi\mathcal{N}$ is independently tunable with $\mathcal{N}_g$. As in the separable case, we then expect $\eta_{\max} = 1/3$. In fact, the result for $\eta_{\max} = 1/3$ carries on at any ratio between capacitances C_{12}, C_1, and C_2 in the Josephson dominated regime, where a multidimensional WKB analysis also shows that the $\mathcal{N}$-dispersion of $\mathcal{E}_0$ is dominated by the two first harmonics with an independently tunable difference between AC shifts [28,43].

The nonreciprocity in the current-voltage characteristics of a Bloch diode is illustrated in Fig. 5 by solving Eq. (1) for the Bloch diode with maximal efficiency $\eta = \frac{1}{3}$ in the Josephson-dominated regime and $\eta = (\sqrt{2}-1)^2$ in the Coulomb-dominated regime. Near voltage thresholds $V_{c\pm}$, the current displays inverse square-root and logarithmic singularities, respectively. Note that this theory neglects interband transitions. In the Josephson-dominated regime,

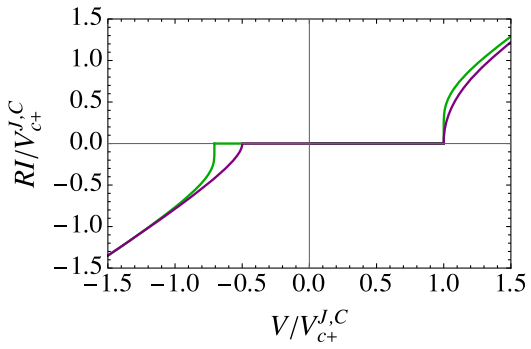

FIG. 5. Nonreciprocal current-voltage characteristics of the Bloch diode described by the ratchet potential of Fig. 3 (purple) and Fig. 4 (green).

this is guaranteed over a large voltage range by the gap between Bloch bands (on the order of the Josephson plasma frequency); in the Coulomb dominated regime, the condition for neglecting Landau-Zener tunneling to the upper bands is $e|V| \ll (E_J^2/E_C)(R/R_Q)$ [26]. Thermal and quantum fluctuations are expected to smooth out the nonreciprocal response at $k_B T \sim eV_{c\pm}$ [44] and $R \sim R_Q$, respectively.

The Bloch diode that we studied is related to the so-called "bifluxon" qubit [45], where a Cooper pair transistor is closed by an inductance to form a flux-tunable loop. The bifluxon provides an example of a "few-body" qubit with more than one degree of freedom in the Hamiltonian that describes it, which allows for suppressing relaxation due to charge or flux noise and dephasing due to flux noise. That protection is expected at $\mathcal{N}_g = \frac{1}{2}$ provided that the device is fully symmetric ($E_{J1} = E_{J2}$ and $C_1 = C_2$) [46]. By contrast, the Bloch diode that we predict is precisely due to the device asymmetry. Conversely, measuring the (disappearance of the) Bloch diode effect may help to tune a device to the most symmetric point, such that at $\mathcal{N}_g = 1/2$ only the double quantum phase slip process ($\propto \cos 4\pi\mathcal{N}$) remains. In practice, however, if the timescale of quasiparticle poisoning is not much larger than the measurement timescale, poisoning events can shift either $\mathcal{N}$ or $\mathcal{N}_g$ by $1/2$. Because of the presence of more than one harmonic, this will generally affect the critical voltages, eventually reducing the Bloch diode efficiency. (In general Bloch diode efficiencies with and without quasiparticle poisoning are not opposite. Therefore, quasiparticle poisoning tends to reduce but not suppress the averaged Bloch diode efficiency.)

Finally, we note that transmission lines formed of a Josephson junction array can be used to realize a highly resistive ohmic environment [23,24,47]. We thus envision that the Bloch diode effect predicted in our Letter could be observed in a purely nondissipative superconducting quantum circuit.

Acknowledgments—T.V. acknowledges insightful discussions with P. Kurilovich, V. Kurilovich, and S. Bosco. M. H. and J. S. M. acknowledge funding from Plan France 2030 through Projects No. NISQ2LSQ ANR-22-PETQ-0006 and No. FERBO ANR-23-CE47-0004.

Data availability—The data that support the findings of this article are openly available [48].

[1] M. Nadeem, M. S. Fuhrer, and X. Wang, The superconducting diode effect, Nat. Rev. Phys. **5**, 558 (2023).

[2] I. Zapata, R. Bartussek, F. Sols, and P. Hänggi, Voltage rectification by a SQUID ratchet, Phys. Rev. Lett. **77**, 2292 (1996).

[3] A. A. Reynoso, G. Usaj, C. A. Balseiro, D. Feinberg, and M. Avignon, Spin-orbit-induced chirality of Andreev states in Josephson junctions, Phys. Rev. B **86**, 214519 (2012).

[4] T. A. Fulton, L. N. Dunkleberger, and R. C. Dynes, Quantum interference properties of double Josephson junctions, Phys. Rev. B **6**, 855 (1972).

[5] R. Seoane Souto, M. Leijnse, and C. Schrade, Josephson diode effect in supercurrent interferometers, Phys. Rev. Lett. **129**, 267702 (2022).

[6] Ya. V. Fominov and D. S. Mikhailov, Asymmetric higher-harmonic SQUID as a Josephson diode, Phys. Rev. B **106**, 134514 (2022).

[7] M. Valentini, O. Sagi, L. Baghumyan, T. de Gijsel, J. Jung, S. Calcaterra, A. Ballabio, J. A. Servin, K. Aggarwal, M. Janik, T. Adletzberger, R. S. Souto, M. Leijnse, J. Danon, C. Schrade, E. Bakkers, D. Chrastina, G. Isella, and G. Katsaros, Parity-conserving Cooper-pair transport and ideal superconducting diode in planar Germanium, Nat. Commun. **15**, 169 (2024).

[8] A. Leblanc, C. Tangchingchai, Z. Sadre Momtaz, E. Kiyooka, J.-M. Hartmann, G. Troncoso Fernandez-Bada, Z. Scherübl, B. Brun, V. Schmitt, S. Zihlmann, R. Maurand, E. Dumur, S. De Franceschi, and F. Lefloch, From nonreciprocal to charge-4e supercurrent in Ge-based Josephson devices with tunable harmonic content, Phys. Rev. Res. **6**, 033281 (2024).

[9] S. Scheidl and V. M. Vinokur, Quantum Brownian motion in ratchet potentials, Phys. Rev. B **65**, 195305 (2002).

[10] K. Hamamoto, T. Park, H. Ishizuka, and N. Nagaosa, Scaling theory of a quantum ratchet, Phys. Rev. B **99**, 064307 (2019).

[11] See Sec. 55 in E. M. Lifshitz and L. P. Pitaevskii, *Statistical Physics, Part 2: Theory of the Condensed State* (Pergamon Press, Oxford, 1980).

[12] A. Schmid, Diffusion and localization in a dissipative quantum system, Phys. Rev. Lett. **51**, 1506 (1983).

[13] J. Hu, C. Wu, and X. Dai, Proposed design of a Josephson diode, Phys. Rev. Lett. **99**, 067004 (2007).

[14] K. Misaki and N. Nagaosa, Theory of the nonreciprocal Josephson effect, Phys. Rev. B **103**, 245302 (2021).

[15] Y. Zhang, Y. Gu, P. Li, J. Hu, and K. Jiang, General theory of Josephson diodes, Phys. Rev. X **12**, 041013 (2022).

[16] D. V. Averin and K. K. Likharev, Single electronics: Correlated transfer of single electrons and cooper pairs in systems of small tunnel junctions, in *Mesoscopic Phenomena in Solids*, edited by B. L. Altshuler, P. A. Lee, and R. A. Webb (Elsevier, New York, 1991).

[17] T. A. Fulton, P. L. Gammel, D. J. Bishop, L. N. Dunkleberger, and G. J. Dolan, Observation of combined Josephson and charging effects in small tunnel junction circuits, Phys. Rev. Lett. **63**, 1307 (1989).

[18] L. J. Geerligs, V. F. Anderegg, J. Romijn, and J. E. Mooij, Single cooper-pair tunneling in small-capacitance jonctions, Phys. Rev. Lett. **65**, 377 (1990).

[19] M. T. Tuominen, J. M. Hergenrother, T. S. Tighe, and M. Tinkham, Experimental evidence for parity-based 2e periodicity in a superconducting single-electron tunneling transistor, Phys. Rev. Lett. **69**, 1997 (1992).

[20] B. Haviland, Y. Pashkin, and L. S. Kuzmin, Measurement of the superconducting single electron transistor in a high impedance environment, Physica (Amsterdam) **203B**, 347 (1994).
[21] A. B. Zorin, S. V. Lotkhov, Yu. A. Pashkin, H. Zangerle, V. A. Krupenin, T. Weimann, H. Scherer, and J. Niemeyer, Highly sensitive electrometers based on single cooper pair tunneling, J. Supercond. **12**, 747 (1999).
[22] S. V. Lotkhov, S. A. Bogoslovsky, A. B. Zorin, and J. Niemeyer, Cooper pair cotunneling in single charge transistors with dissipative electromagnetic environment, Phys. Rev. Lett. **91**, 197002 (2003).
[23] M. Watanabe, Single-electron transistors in electromagnetic environments, Phys. Rev. B **69**, 094509 (2004).
[24] S. Corlevi, W. Guichard, F. W. J. Hekking, and D. B. Haviland, Phase-charge duality of a Josephson junction in a fluctuating electromagnetic environment, Phys. Rev. Lett. **97**, 096802 (2006).
[25] K. K. Likharev and A. B. Zorin, Theory of the Bloch-wave oscillations in small Josephson junctions, J. Low Temp. Phys. **59**, 347 (1985).
[26] D. V. Averin, A. B. Zorin, and K. K. Likharev, Bloch oscillations in small Josephson junctions, Zh. Eksp. Teor. Fiz. **88**, 692 (1985) [Sov. Phys. JETP **61**, 407 (1985)], https://jetp.ras.ru/cgi-bin/e/index/e/61/2/p407?a=list.
[27] F. Kaap, C. Kissling, V. Gaydamachenko, L. Grünhaupt, and S. Lotkhov, Demonstration of dual Shapiro steps in small Josephson junctions, Nat. Commun. **15**, 8726 (2024).
[28] F. Kaap, D. Scheer, F. Hassler, and S. Lotkhov, Synchronization of Bloch oscillations in a strongly coupled pair of small Josephson junctions: Evidence for a Shapiro-like current step, Phys. Rev. Lett. **132**, 027001 (2024).
[29] R. S. Shaikhaidarov, K. Ho Kim, J. Dunstan, I. Antonov, D. Golubev, V. N. Antonov, and O. V. Astafiev, Quantized current steps due to the synchronization of microwaves with Bloch oscillations in small Josephson junctions, Nat. Commun. **15**, 9326 (2024).
[30] M. A. Sillanpää, T. Lehtinen, A. Paila, Yu. Makhlin, L. Roschier, and P. J. Hakonen, Direct observation of Josephson capacitance, Phys. Rev. Lett. **95**, 206806 (2005).
[31] T. Duty, G. Johansson, K. Bladh, D. Gunnarsson, C. Wilson, and P. Delsing, Observation of quantum capacitance in the cooper-pair transistor, Phys. Rev. Lett. **95**, 206807 (2005).
[32] J. Koch, T. M. Yu, J. Gambetta, A. A. Houck, D. I. Schuster, J. Majer, A. Blais, M. H. Devoret, S. M. Girvin, and R. J. Schoelkopf, Charge-insensitive qubit design derived from the Cooper pair box, Phys. Rev. A **76**, 042319 (2007).
[33] D. A. Ivanov, L. B. Ioffe, V. B. Geshkenbein, and G. Blatter, Interference effects in isolated Josephson junction arrays with geometric symmetries, Phys. Rev. B **65**, 024509 (2001).
[34] J. R. Friedman and D. V. Averin, Aharonov-Casher-effect suppression of macroscopic tunneling of magnetic flux, Phys. Rev. Lett. **88**, 050403 (2002).
[35] J. Zinn-Justin, Multi-instanton contributions in quantum mechanics, Nucl. Phys. **B192**, 125 (1981).
[36] T. Vakhtel, P. D. Kurilovich, M. Pita-Vidal, A. Bargerbos, V. Fatemi, and B. van Heck, Tunneling of fluxons via a Josephson resonant level, Phys. Rev. B **110**, 045404 (2024).
[37] W. Ardati, S. Léger, S. Kumar, V. N. Suresh, D. Nicolas, C. Mori, F. D'Esposito, T. Vakhtel, O. Buisson, Q. Ficheux, and N. Roch, Using bifluxon tunneling to protect the fluxonium qubit, Phys. Rev. X **14**, 041014 (2024).
[38] P. A. Volkov, E. Lantagne-Hurtubise, T. Tummuru, S. Plugge, J. H. Pixley, and M. Franz, Josephson diode effects in twisted nodal superconductors, Phys. Rev. B **109**, 094518 (2024).
[39] T. Vakhtel and B. van Heck, Quantum phase slips in a resonant Josephson junction, Phys. Rev. B **107**, 195405 (2023).
[40] A. Mert Bozkurt and V. Fatemi, Josephson tunnel junction arrays and Andreev weak links: Linked by a single energy-phase relation, arXiv:2408.06462.
[41] P. D. Kurilovich, V. D. Kurilovich, V. Fatemi, M. H. Devoret, and L. I. Glazman, Microwave response of an Andreev bound state, Phys. Rev. B **104**, 174517 (2021).
[42] U. Güngördü, R. Ruskov, S. Hoffman, K. Serniak, A. J. Kerman, and C. Tahan, Quantum dynamics of semiconductor quantum dot, Phys. Rev. B **111**, 214503 (2025).
[43] A. G. Semenov, A. Latyshev, and A. D. Zaikin, Quantum Coulomb drag mediated by cotunneling of fluxons and Cooper pairs, Phys. Rev. Lett. **134**, 086001 (2025).
[44] The details of thermal smearing could be addressed numerically within a standard Fokker-Planck method by incorporating thermal noise in Eq. (1). This question is left for future study.
[45] K. Kalashnikov, W. T. Hsieh, W. Zhang, W.-S. Lu, P. Kamenov, A. Di Paolo, A. Blais, M. E. Gershenson, and M. Bell, Bifluxon: Fluxon-parity-protected superconducting qubit, PRX Quantum **1**, 010307 (2020).
[46] A. Maassen van den Brink, Comment on, "Aharonov–Casher-effect suppression of macroscopic tunneling of magnetic flux," arXiv:cond-mat/0206218.
[47] N. A. Masluk, I. M. Pop, A. Kamal, Z. K. Minev, and M. H. Devoret, Microwave characterization of Josephson junction arrays: Implementing a low loss superinductance, Phys. Rev. Lett. **109**, 137002 (2012).
[48] M. Houzet, T. Vakhtel, and J. S. Meyer (2025), 10.5281/zenodo.17624156.

End Matter

Appendix A: "Double quantum phase slip" amplitude—Here we derive the exponentially small dispersion of the ground state energy of a Cooper pair box, which is described by the Hamiltonian (6), in the Josephson-dominated regime up to the second harmonic in gate charge $\mathcal{N}$; see Eq. (11).

For this we note that, up to a gauge transformation, the eigenenergies of a Cooper pair box are defined by the following eigenproblem:

$$\left[-E_C\frac{d^2}{d\varphi^2}-E_J\cos\varphi\right]\psi(\varphi)=E\psi(\varphi), \tag{A1}$$

where the wave function $\psi(\varphi)$ must satisfy the twisted periodic boundary condition

$$\psi(\varphi+2\pi)=e^{-i2\pi\mathcal{N}}\psi(\varphi). \tag{A2}$$

Here for simplicity we omit the index $k=1,2$ used in the main text. Our strategy to obtain Eq. (11) is to solve perturbatively a transcendental equation solved by $E(\mathcal{N})$. To find that equation, we determine the most general forms of the solutions of Eq. (A1) for phases in the vicinity of multiples of 2π, where $\psi(\varphi)$ has most of its support at $E_J \gg E_C$, as well as in the classically forbidden regions, and then match them in a common range in φ, where both of these solutions are defined.

Let us first consider the vicinity of $\varphi=0$. We may use an harmonic approximation of the Josephson potential, $\cos\varphi\approx 1-\varphi^2/2$, and rescaled variables $\varphi=x\sqrt[4]{E_C/2E_J}$ and $E=-E_J+\hbar\omega(p+1/2)$ with plasma frequency $\hbar\omega=\sqrt{2E_JE_C}$, to find that Eq. (A1) reduces to

$$\left(\frac{d^2}{dx^2}+p+\frac{1}{2}-\frac{x^2}{4}\right)\psi(x)=0. \tag{A3}$$

Its most general solution is expressed in terms of parabolic cylinder functions $D_p(x)$,

$$\psi(x)=A_1D_p(x)+A_2D_p(-x), \tag{A4}$$

where A_1 and A_2 are two constants to be determined. The asymptotes of Eq. (A4) at $x\gg 1$ and $-x\gg 1$ are

$$\psi(x)\approx(A_1+A_2e^{-i\pi p})x^pe^{-x^2/4}-A_2\frac{\sqrt{2\pi}}{\Gamma(-p)}\frac{e^{x^2/4}}{x^{p+1}} \tag{A5}$$

and

$$\psi(x)\approx(A_1e^{i\pi p}+A_2)(-x)^pe^{-x^2/4}-A_1\frac{\sqrt{2\pi}}{\Gamma(-p)}\frac{e^{x^2/4}}{(-x)^{p+1}}, \tag{A6}$$

respectively. Note that the condition $|x|\gg 1$ is still compatible with $|\varphi|\ll 1$ used in the harmonic approximation for the Josephson potential at $E_J\gg E_C$. For $\psi(x)$ to remain localized near $\varphi=0$, the last term in Eqs. (A5) and (A6) should be suppressed. Given the properties of the Euler function $\Gamma(-p)$, this requires that p should be close to a positive integer m, in agreement with the expectation for the eigenenergies of a quantum harmonic oscillator,

$$E_m=-E_J+\hbar\omega\left(m+\frac{1}{2}\right)-\frac{E_C}{8}\left(m^2+m+\frac{1}{2}\right). \tag{A7}$$

Here we dispense with the derivation of a small, $\mathcal{N}$-independent anharmonic correction to the eigenenergies captured by the last term of Eq. (A7) [32], which can be obtained by expanding $\cos\varphi$ up to quartic order in φ.

Equivalent solutions with the same eigenspectrum can be found by expanding the Josephson potential near $\varphi=2\pi n$ with any integer n. It is their hybridization that results in the formation of Bloch bands. To proceed further, we then express the most general form of the wave function in an interval between two minima of the Josephson potential, say for φ such that $\varphi\gg\sqrt[4]{E_C/E_J}$ and $2\pi-\varphi\gg\sqrt[4]{E_C/2E_J}$, using the WKB approximation in the classically forbidden regions,

$$\psi(\varphi)\approx\frac{B_1}{\sqrt{\kappa(\varphi)}}e^{-\int_\pi^\varphi d\varphi'\kappa(\varphi')}+\frac{B_2}{\sqrt{\kappa(\varphi)}}e^{\int_\pi^\varphi d\varphi'\kappa(\varphi')}. \tag{A8}$$

Here $\kappa(\varphi)=\sqrt{(-E_J\cos\varphi-E)/E_C}$, and B_1 and B_2 are two other constants to be determined. [The choice of π as a bound in the integrals that appear in Eq. (A8) was made for convenience; another choice could be absorbed in B_1 and B_2.] As φ remains away from the classical turning points [where the argument in $\kappa(\varphi)$ would vanish], we may approximate

$$\kappa(\varphi)\approx\sqrt{\frac{2E_J}{E_C}}\sin(\varphi/2)-\frac{p+\frac{1}{2}}{2\sin(\varphi/2)}, \tag{A9}$$

$$\int_\pi^\varphi d\varphi'\kappa(\varphi')\approx-\sqrt{\frac{8E_J}{E_C}}\cos\frac{\varphi}{2}-\left(p+\frac{1}{2}\right)\ln\tan\frac{\varphi}{4}. \tag{A10}$$

As a result, Eq. (A8) further simplifies to

$$\psi(\varphi)\approx\frac{B_1}{\sqrt{\sin(\varphi/2)}}\left(\tan\frac{\varphi}{4}\right)^{p+\frac{1}{2}}e^{\sqrt{\frac{8E_J}{E_C}}\cos(\varphi/2)}+\frac{B_2}{\sqrt{\sin(\varphi/2)}}\left(\tan\frac{\varphi}{4}\right)^{-p-\frac{1}{2}}e^{-\sqrt{\frac{8E_J}{E_C}}\cos(\varphi/2)}, \tag{A11}$$

up to a common constant absorbed in B_1 and B_2.

In particular, the asymptote of Eq. (A11) at $\sqrt[4]{E_C/E_J}\ll\varphi\ll 1$ has identical parametric dependence on $\varphi\propto x$ as in Eq. (A5). This allows for identifying two relations between coefficients A_1, A_2, B_1, and B_2:

$$A_1+A_2e^{-i\pi p}=\frac{B_1}{\sqrt{2}}\left(\frac{E_C}{2^9E_J}\right)^{p/4}e^{\sqrt{8E_J/E_C}}, \tag{A12}$$

$$A_2\frac{\sqrt{2\pi}}{\Gamma(-p)}=-\frac{B_2}{\sqrt{2}}\left(\frac{E_C}{2^9E_J}\right)^{-(p+1)/4}e^{-\sqrt{8E_J/E_C}}. \tag{A13}$$

Similarly, Eq. (A11) yields an asymptote at $\sqrt[4]{E_C/2E_J}\ll 2\pi-\varphi\ll 1$, which can be put in correspondence with Eq. (A6) using the periodic boundary condition

given by Eq. (A2). This yields two additional relations:

$$A_1 e^{i\pi p} + A_2 = \frac{B_2}{\sqrt{2}} \left(\frac{E_C}{2^9 E_J}\right)^{p/4} e^{-\sqrt{8E_J/E_C}} e^{-2i\pi\mathcal{N}}, \quad \text{(A14)}$$

$$A_1 \frac{\sqrt{2\pi}}{\Gamma(-p)} = -\frac{B_1}{\sqrt{2}} \left(\frac{E_C}{2^9 E_J}\right)^{-(p+1)/4} e^{\sqrt{8E_J/E_C}} e^{-2i\pi\mathcal{N}}. \quad \text{(A15)}$$

The linear system of Eqs. (A12)–(A15) yields the sought-after transcendental equation solved by $\delta E_m \equiv E - E_m = \hbar\omega(p-m)$ with p close to integer m:

$$2\cos 2\pi\mathcal{N} = \frac{\sqrt{2\pi}}{\Gamma(-p)} \left(\frac{E_C}{2^9 E_J}\right)^{p/2+1/4} e^{\sqrt{32E_J/E_C}}. \quad \text{(A16)}$$

Using $1/\Gamma(-p) \approx (-1)^{m+1} m![(p-m) + \psi_0(m+1)(p-m)^2]$ at $|p-m| \ll 1$, where $\psi_0(m)$ is the digamma function, we expand Eq. (A16) to find

$$\delta E_m = -\lambda_m \cos 2\pi\mathcal{N} + \frac{\lambda_m^2}{2\hbar\omega} \ln\left(\frac{2^4\hbar\omega}{e^{\psi_0(m+1)} E_C}\right) \cos^2 2\pi\mathcal{N}. \quad \text{(A17)}$$

with

$$\frac{\lambda_m}{\hbar\omega} = \frac{(-1)^m}{m!} \sqrt{\frac{2}{\pi}} \left(\frac{2^9 E_J}{E_C}\right)^{m/2+1/4} e^{-\sqrt{32E_J/E_C}}. \quad \text{(A18)}$$

At $m = 0$ with $\psi(1) = -\gamma$ where γ is Euler's constant, Eq. (A17) reproduces Eq. (11).

Appendix B: Diode efficiency in a hybrid regime—Here we provide the diode efficiency in a hybrid regime where one of the junctions is in the Coulomb dominated regime (say $E_{J1} \ll E_{C1}$) and the other one is in the Josephson dominated regime (say $E_{J2} \gg E_{C2}$). If $y \equiv e^2/(\pi^2 C_1 \lambda_2) > 1$,

$$\frac{eV^{>}_{c\pm}}{\pi\lambda_2} = \pm\pi y + \sin 2\pi\mathcal{N}_g, \quad \text{(B1)}$$

yielding maximal diode efficiency $\eta_{\max} = 1/\pi \approx 0.32$ at $\mathcal{N}_g = \frac{1}{4}$ and $y \to 1$. If $y < 1$, $V_{c+} = V^{<}_{c+}$ and $V_{c-} = \min(V^{>}_{c-}, V^{<}_{c-})$ with

$$\frac{eV^{<}_{c\pm}}{\pi\lambda_2} = \pm[\sqrt{1-y^2} + y(\pi - \arccos y)] + 2\pi y\mathcal{N}_g, \quad \text{(B2)}$$

yielding maximal diode efficiency $\eta_{\max} \approx 0.60$ at $y \approx 0.43$ and $\mathcal{N}_g \approx 0.39$.